COST STSM FP1006-13034 Scientific Report

STSM title: Plasma modification of wood-siloxane composites

STSM applicant: Daniel Van Opdenbosch, Fachgebiet Biogene Polymere, Technische Universität München

Host: Gheorghe Dinescu, National Institute for Laser, Plasma and Radiation Physics, Magurele Bucharest

Period: April 2013

Purpose of the STSM

The purpose of this STSM was to assess the possibility to improve the effectivity of the wood treatment with siloxanes by additional plasma treatment to impart water-repelling properties.

Abstract

Wood was treated by combinations of liquid impregnation or gas-phase impregnation with the siloxane precursor phenyltrimethoxysilane (PTMOS) and prior argon plasma activation or subsequent curing to improve their water-repelling properties. It was found that the activation increases the resulting antishrink-efficiency of the liquid impregnated wood by 8 %. Further experiments showed that the use of an appropriate solvent is critical for a deposition within the cell walls and that even 4 wt% of PTMOS already impart a significant water-repellence. Fourier-transform infrared analysis showed the activation of the wood surface and the inclusion of the precursor in the treated wood samples. It further showed that the degree of hydrolysis of the precursors was increased both by plasma activation and curing. This in turn is directly attributed to the increased ASE of the wood. Gas deposition did not lead to significant material deposition or improved properties of the resulting composites.

Introduction

The treatment of wood by liquid impregnation of hydrophobic silicon compounds is a known technique to improve its water-repelling properties [1]. In this context, the effectivity of phenyl-substituted alkoxysilanes has recently been demonstrated [2]. The resulting hydrophobisation was due to the combined effects of cell wall pore filling, inclusion of highly hydrophobic aromatic groups and bonding to wood hydroxyl groups. However, such processing relies on the impregna-

tion of entire samples under vacuum and the subsequent time-consuming drying of the sample. Further, it was found that the impregnated precursors were not fully condensed after drying and that there was loss of precursor during processing due to evaporation of uncondensed species.

Plasma treatment is a powerful tool to change surface properties over a wide range [3]. Accordingly, it has been used to improve the water-repelling properties of wood [4]. However, in application this requires more than surface hydrophobisation. An important property of a protective wood treatment is imparting a high antishrink efficiency, which can only be achieved by bulk treatment of either the wood cell lumen or the cell walls, of which the latter is the more efficient [5,6]. We therefore combined plasma and siloxane treatments to assess the possibility to combine the advantages of the two processes, namely rapid surface activation or precursor curing and bulk modification. Three different principal processing routes were assessed. The first used plasma activation of the wood surface to increase its reactivity and subsequent liquid impregnation of precursor solutions. The activated surface is expected to show increased wetting and also reactivity similar to a chemical pretreatment [7]. The second used liquid impregnation followed by plasma treatment to condense the precursor in the samples, thereby reducing the time needed to dry the impregnated precursor. The third used precursor deposition from the gas phase to provide a rapid means of wood treatment, improving on prior treatments by using a different direction of the gas stream and a highly hydrophobic precursor [8].

Materials and methods

Wood samples, either Kraft-pulped pine *(Pinus radiata)* fibres with Kappa number 25 or organically extracted (2:1 ethanol-toluene/ethanol, 6 h each) pine *(Pinus sylvestris)* pieces were subjected to combinations of plasma activation, liquid impregnation, plasma curing, plasma and gas deposition techniques with the siloxane precursor phenyltrimethoxysilane (PTMOS), Figure 1. The fibres were dispersed first in water and then in ethanol to ensure good separation after drying. The pieces were cut along the RT plane (i.e. perpendicular to the grain) with a circular saw.

All samples are named according to the scheme $^{X}Y_{Z}$ where X describes the processing key, Y the precursor type and Z the substrate. Substrates were either pine wood pieces (Z=W) or Kraft-pulp fibres (Z=KPF). Due to their respective applicability to several processing routes, the general control group comprised two sample types: $Ref_{KPF/W}$ and $^{P}Ref_{KPF/W}$, meaning untreated and plasma treated KPF and wood, respectively. As an example, $^{PL}PTMOS_{W}$ indicates plasma treatment followed by liquid impregnation of PTMOS, performed on wood pieces.

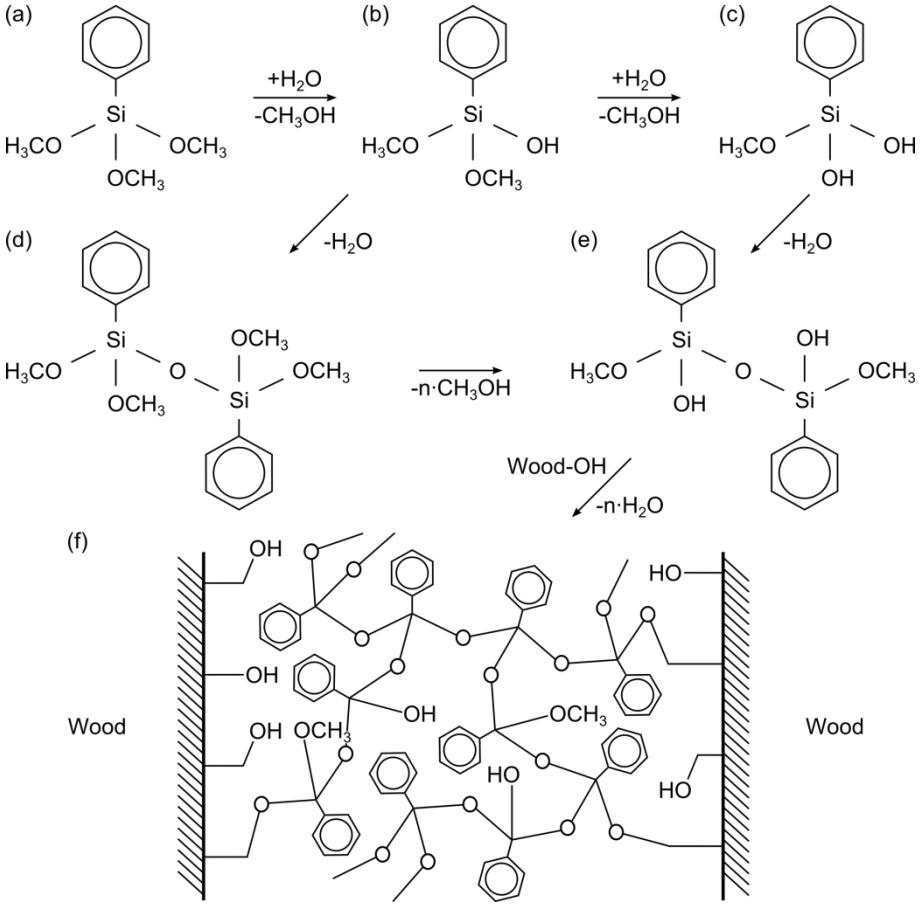

Figure 1: (a) Phenyltrimethoxysilane and its (b) single or (c) multiple hydrolysed forms condense under loss of water either (d) immediately or (e) after further hydrolysis. Condensation with wood hydroxyl groups, forming (f) a network under loss of water, has been shown to occur. This network is formed between the cellulose fibrils in the cell walls, preventing water uptake [2].

Three different principal methods were assessed, as listed in Table 1 and described in the following:

1a) Plasma activation followed by liquid impregnation. Plasma activation was carried out at a power of 5 W, vacuum pressure of $5 \cdot 10^{-2}$ mbar, work pressure of 10^{-1} mbar, argon flow of 50 scc/m for 5 min. Samples were liquid impregnated in a solution of 1.28 g TEOS, 1.22 g PTMOS, or 1.48 g PTEOS per 1 g wood, dissolved in 75 g EtOH. To remove air from the samples, a vacuum of 8.5 mbar was applied for 5 min. Subsequently, the samples were dried on a heating plate at 50 °C for 12 h, 75 °C for 4 h and 105 °C for 4 h. Their processing key is X=PL (plasma treated and liquid impregnated).

1b) Plasma activation followed by solventless liquid impregnation. Plasma activation was carried out according to 1a) Samples were liquid impregnated by 1.28 g TEOS, 1.22 g PTMOS, or 1.48 g PTEOS per 1 g wood. Subsequently, the samples were dried on a hot plate at 50 °C for 12 h,

75 °C for 4 h and 105 °C for 4 h. Their processing key is X=PLNS (plasma treated and liquid impregnated, no solvent).

2a) Liquid impregnation followed by plasma curing. Liquid impregnation was carried out according to 1a). Plasma curing was performed at a power of 50 W, vacuum pressure of $5 \cdot 10^{-2}$ mbar, work pressure of 10^{-1} mbar, argon flow of 30 scc/m for 10 min. Their processing key is X=LP (liquid impregnated and plasma treated).

2b) Liquid impregnation followed by vacuum drying and plasma curing. Liquid impregnated samples were taken from the impregnation solution and then subjected to vacuum to remove the solvent. This was followed by immediate plasma treatment according to 2a). Their processing key is X=LDOP (liquid impregnated, dried outside precursor solution and plasma-treated).

3a) Plasma activation and simultaneous precursor deposition. Before reaching the plasma chamber, the argon stream was directed through the liquid precursor heated to 50 °C at a flow rate of 30 scc/m. The precursor and argon plasma was created at a power of 20 W and a work pressure of 10^{-1} mbar. Their processing key is X=P (one-step plasma-assisted deposition).

3b) Plasma activation and subsequent gas-phase precursor deposition. Samples were activated according to 1b) and subjected to a mixture of argon and precursor molecules according to 3a) and at a pressure of 10^{-1} mbar. Their processing key is X=PG (plasma activation followed by gas-phase deposition).

The specific control samples $^{L}PTMOS_{KPF/W}$, $^{LNS}PTMOS_{KPF/W}$, $^{LDO}PTMOS_{KPF/W}$ and $^{G}PTMOS_{KPF/W}$ were prepared, omitting plasma treatments.

Relative dimensional (Δax, Δrad, Δtan in the axial, radial and tangential wood directions) and mass changes (weight percentage gains, WPG) during treatment were determined by measuring with a sliding calliper and a precision scale (Adventurer Pro, Ohaus, United States of America). All dimensional and mass changes were corrected for the native wood shrinkages during drying and their moisture contents (Δax -0.68±0.07, Δrad -1.01±0.04, Δtan -1.89±0.16, EMC 6.32±0.16). The initial strut densities and porosities of the templates were determined by helium pycnometry (AccuPyc 1330, Particle and Surface Sciences, Gosford, Australia). The antishrink efficiencies of treated wood pieces (ASE) were determined from their wet and dry volumes by immersing the wood cubes in distilled water at 10 mbar for 0.5 h and then at ambient pressure for 24 h. The wet specimens were dried at 105 °C. The ASEs were then calculated from the dimensions in their wet and dry states. Contact angle (CA) measurement was performed with a dedicated device (CAM 101, KSV Instruments, Espoo, Finland) on four drops, deposited on the radial/tangential (RT) plane each. If the drops were absorbed into the wood in less than 1 min,

the time for complete absorption, named contact time (CT) was determined as well. The ash determination was performed according to TAPPI standard T413. The thermal properties of selected samples were assessed on a combined thermogravimetric and differential thermal analysis (TGA/DTA) machine (Diamond, Perkin Elmer, Waltham, United States of America). The localisation of the embedded precursors was determined by light microscopy (RML 5, Mikroskop Technik Rathenow, Germany) of treated and ashed fibres. Chemical changes to the samples during treatment were determined by Fourier-transform infrared spectroscopy (FTIR, 6300, Jasco, United States of America) on KPF.

Table 1: Samples prepared during the investigation. Groups of samples were prepared by (L) liquid impregnation, (LNS) liquid impregnation with no solvent, (LDO) liquid impregnation dried outside the precursor solution, (G) gas-phase deposition, with or without (P) plasma activation or curing on pine (KPF) Kraft pulp fibres and (W) wood pieces.

Name	Template	Plasma	Liquid precursor	Gas precursor	Precursor before, in or after plasma	Drying
$^{P}Ref_{KPF/W}$	KPF/W	low vacuum	no	no	/	/
$^{L}PTMOS_{KPF?/W}$	KPF/W	/	yes	no	/	in precursor
$^{LNS}PTMOS_{W}$	W	/	no solvent	no	/	outside precursor
$^{LDO}PTMOS_{KPF?/W}$	KPF/W	/	yes	no	/	outside precursor
$^{PL}PTMOS_{KPF?/W}$	KPF/W	low vacuum	yes	no	after	in precursor
$^{PLNS}PTMOS_{W}$	W	low vacuum	no solvent	no	after	in precursor
$^{LP}PTMOS_{KW}$	W	low vacuum	yes	no	before	in precursor
$^{LDOP}PTMOS_{KPF/W}$	KPF/W	low vacuum	yes	no	before	outside precursor
$^{G10/G30}PTMOS_{W}$	W	low vacuum	no	10/30 mins	in	/
$^{P10/P30}PTMOS_{W}$	W	low vacuum	no	10/30 mins	in	/
$^{PG10/G30}PTMOS_{W}$	W	low vacuum	no	10/30 mins	after	/

Results

Antishrink efficiency

The parameters that are most important to assess the water-repelling properties of treated wood samples are arguably their ASE and CA. The former were increased by treatment with siloxane precursor solutions, Figure 2. The liquid impregnation of $^{L}PTMOS_{W}$ increased the ASE of the wood. The obtained value of 17 % was used as the control in this study and was considerably increased by prior plasma activation in $^{PL}PTMOS_{W}$. The slight increase by plasma curing in $^{LP}PTMOS_{W}$ is considered to be the same as in $^{L}PTMOS_{W}$. The strongly swollen plasma activation control sample $^{P}Ref_{W}$ was cracked after drying, preventing measurement of the ASE. Control samples $^{LDO}PTMOS_{W}$ and the immediately plasma-cured $^{LDOP}PTMOS_{W}$ showed an even higher ASE as samples $^{LNS}PTMOS_{W}$ $^{PLNS}PTMOS_{W}$, which were treated without the use of a solvent. The samples treated by gas deposition showed no significant ASE.

Contact angles

The organically extracted wood pieces Ref_{W} used in this work showed CA to water of 84.00° and CT of 25.16 s. By contrast, water was taken up immediately by the plasma pretreated control samples $^{P}Ref_{W}$. It could be shown that all treatments involving impregnation of liquid siloxane precursors increased the contact angles of the resulting wood composites, Figure 3. Notably, the samples impregnated without the use of a solvent, $^{LNS}PTMOS_{W}$ and $^{PLNS}PTMOS_{W}$, yielded similar contact angles as $^{L}PTMOS_{W}$.

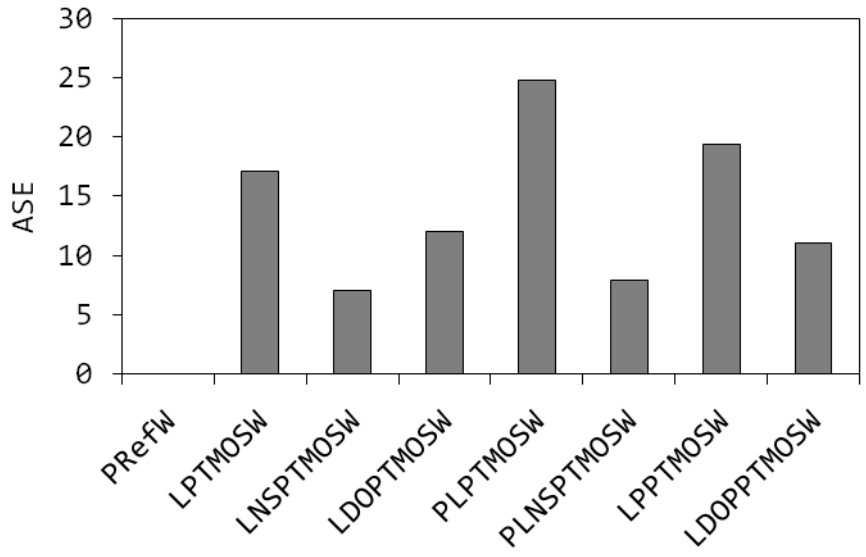

Figure 2: ASE of the treated wood pieces, illustrating the increased effectiveness of plasma pretreatment. Samples that were cracked from drying stresses are named, but results omitted.

Plasma activation followed by liquid impregnation (^{PL}PTMOS$_W$) also yielded the same contact angle as ^{L}PTMOS$_W$. In case of the plasma-cured sample ^{LP}PTMOS$_W$, the increase compared to the wood reference was about 15°, half the increase determined for ^{L}PTMOS$_W$, ^{LNS}PTMOS$_W$, ^{PL}PTMOS$_W$ and ^{PLNS}PTMOS$_W$. By measuring the contact angle (92°) and -time (5 s) of freshly dried wood as a control, it could be shown that this was not due to the drying of the wood from its original moisture content. Since ^{LP}PTMOS$_W$ was prepared in the same way as ^{L}PTMOS$_W$ but with subsequent plasma treatment, its contact angle is considered to be lowered from that of ^{L}PTMOS$_W$. The samples dried outside the precursor solution without or with subsequent plasma curing, ^{LDO}PTMOS$_W$ and ^{LDOP}PTMOS$_W$, both had the same contact angles as ^{LP}PTMOS$_W$.

Samples treated by deposition from the gas phase showed similar contact angles and -times as Ref$_W$. They increased slightly with increased treatment time, as seen from the comparison of ^{G10}PTMOS$_W$ and ^{G30}PTMOS$_W$. The same was observed from plasma-deposition ($^{P10/30}$PTMOS$_W$), but not when gas-phase deposition was preceded by plasma treatment ($^{PG10/30}$PTMOS$_W$). In this case, the contact angles could not be determined and the –times were in the order of 20 ms.

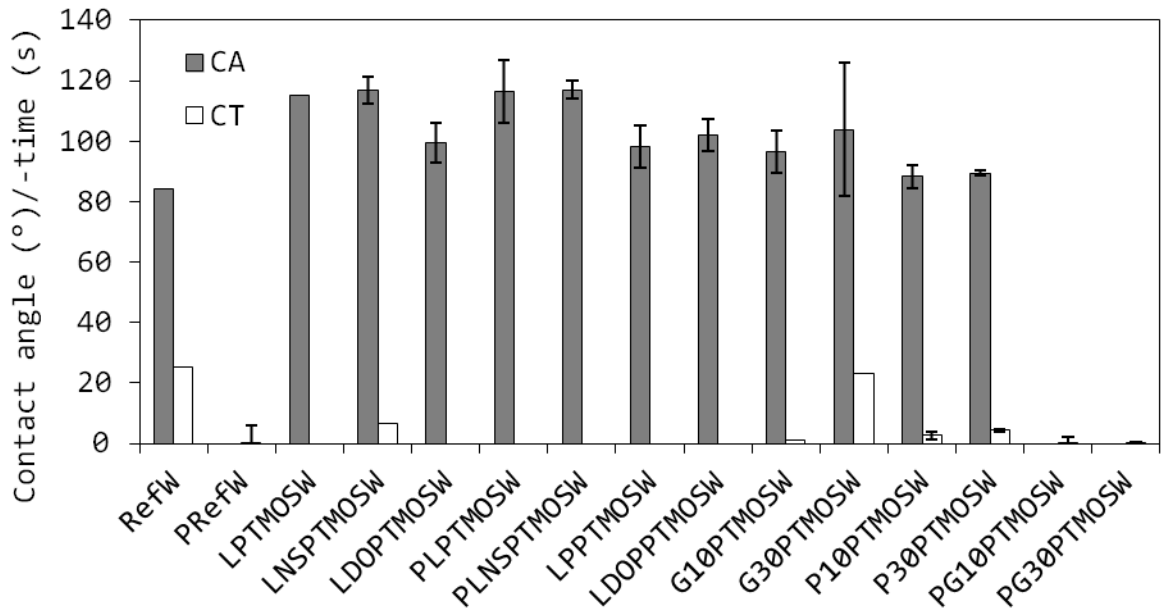

Figure 3: Contact angles and -times of the treated wood pieces named in Table 1, showing that high contact angles were obtained by plasma activation and solventless impregnations.

Dimensional changes

The initial total porosity of the extracted and dried pine wood templates was 66.5±1.5 %, as determined by comparison of the geometrical and strut density of 14 pieces of pine wood. Drying in the precursor solution (^{L}PTMOS$_W$, ^{PL}PTMOS$_W$ and ^{LP}PTMOS$_W$) resulted in the highest mass and volume increases, Figure 4. Control samples ^{LNS}PTMOS$_W$ and ^{LDO}PTMOS$_W$ both showed a

low mass increase during treatment. However, the volume increases of the latter were comparatively high. The plasma-cured equivalents $^{PLNS}PTMOS_W$ and $^{LDOP}PTMOS_W$ had similar dimensional changes, but with lower mass increase. The amount of precursor deposited by the various assessed gas-deposition routes was, even after 120 minutes of treatment, less than the measurement uncertainty of the scale and calliper, which was in turn further exacerbated by the fact that each measurement was corrected for the native wood shrinkages.

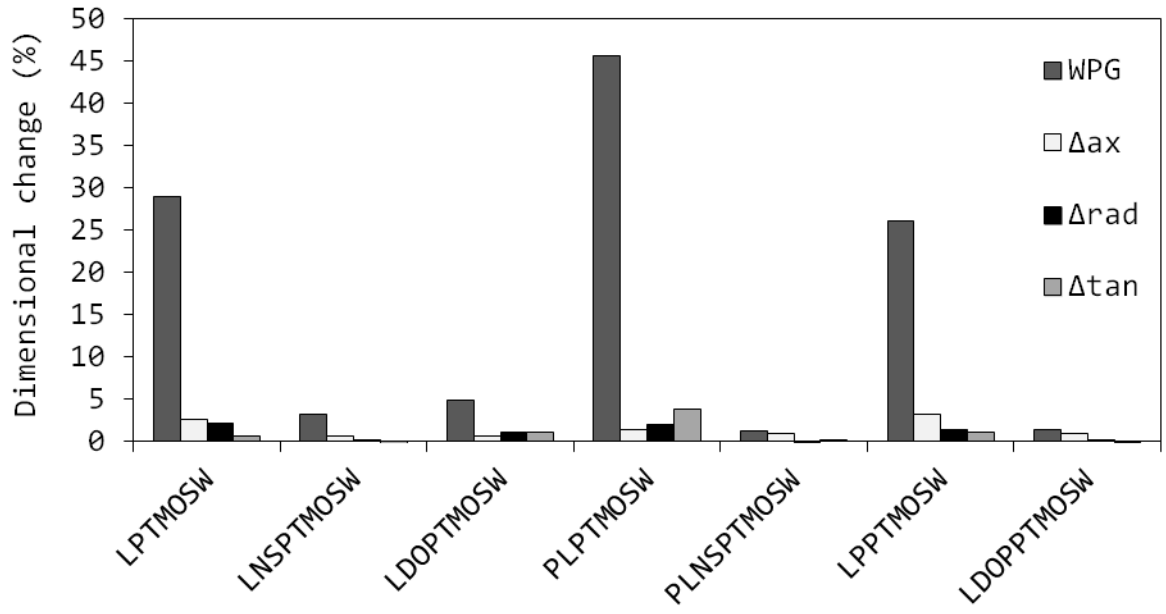

Figure 4: Dimensional changes of treated wood pieces showing that drying in the precursor solution results in the largest mass and volume increases during treatment.

Weight percentage gains of fibres

The mass increases of Kraft-pulped fibres dried in the ethanolic precursor solutions differed by as much as 100 %, Figure 5. Notably, and contrary to the observations on wood pieces, the WPG of $^{PL}PTMOS_{KPF}$ were lower than those of the reference $^{L}PTMOS_{KPF}$ and $^{LP}PTMOS_{KPF}$. On the other hand, the WPG of $^{LNS}PTMOS_{KPF}$ and $^{LDO}PTMOS_{KPF}$ were higher than observed on wood pieces. Samples prepared on non-dispersed fibres, marked with an underline, showed significantly lowered WPG.

Ash contents of fibres

The ash contents of all liquid impregnated samples drying in the precursor solution were the same at 13 %, Figure 6. $^{LDO}PTMOS_{KPF}$ and the samples prepared on non-dispersed fibres expectedly showed comparatively lowered ash contents.

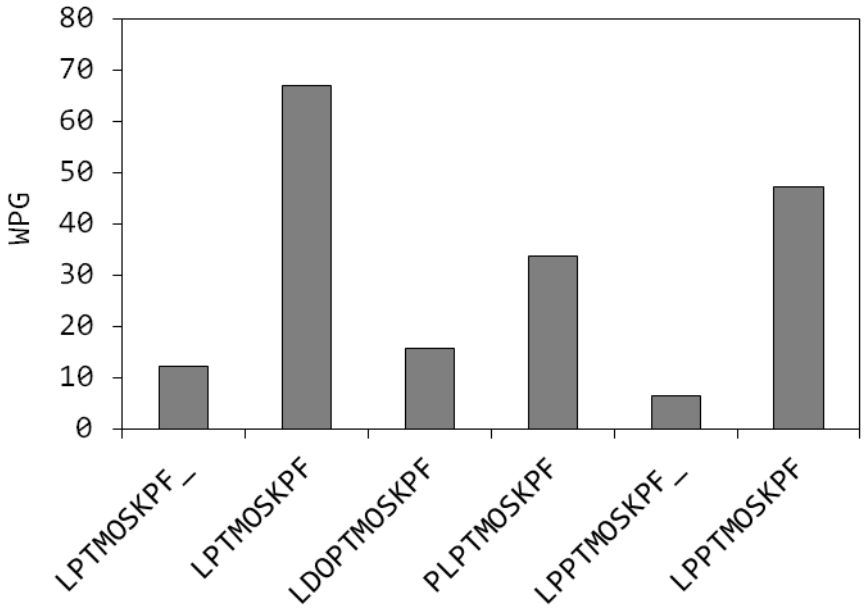

Figure 5: WPG of treated Kraft-pulped wood fibres, showing varying mass increases during treatments. Experiments followed by an underline were conducted on pulp aggregates and illustrate the need for well-dispersed fibres to achieve high deposition rates.

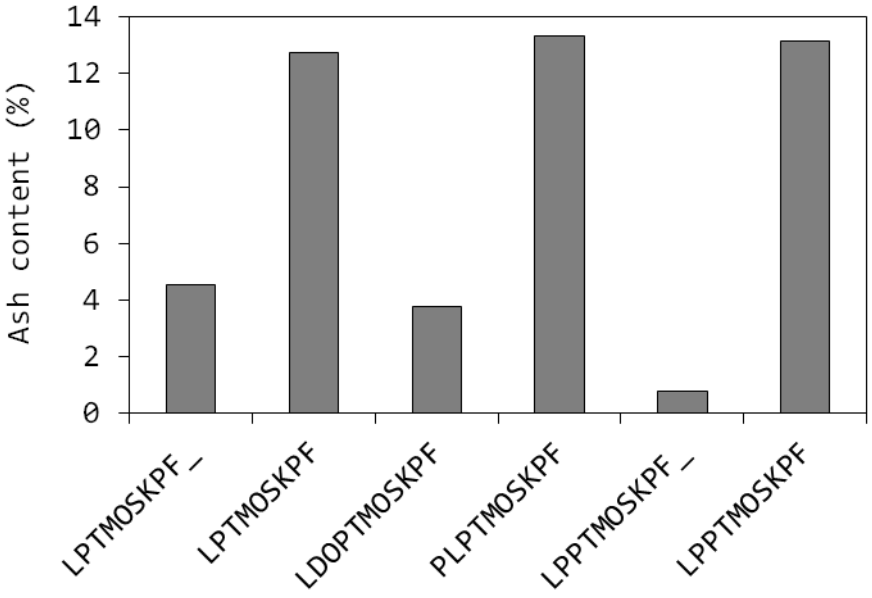

Figure 6: Ash contents of treated Kraft-pulped wood fibres showing that the total amount of deposited precursor is similar for all liquid impregnations dried in the precursor solution. Experiments followed by an underline were conducted on pulp aggregates.

Thermal analysis

Thermal analysis of untreated fibres and the fibres from processes drying in the precursor solution, $^{L}PTMOS_{KPF}$, $^{L}PTMOS_{KPF}$ and $^{L}PTMOS_{KPF}$, confirmed the native ash content of the Kraft-pulp fibres of 0.23±0.01 %. It also confirmed the ash contents of the treated fibres of 13 % determined by conventional ashing, Figure 7. Notably, a mass loss starting at 160 °C can be observed in the curve of sample $^{L}PTMOS_{KPF}$. It points to the evaporation of incompletely condensed PTMOS precursor molecules, which have a boiling point of 175 °C [2]. However, the residual mass of $^{L}PTMOS_{KPF}$ was not significantly lowered and in agreement with ash determinations (Figure 5).

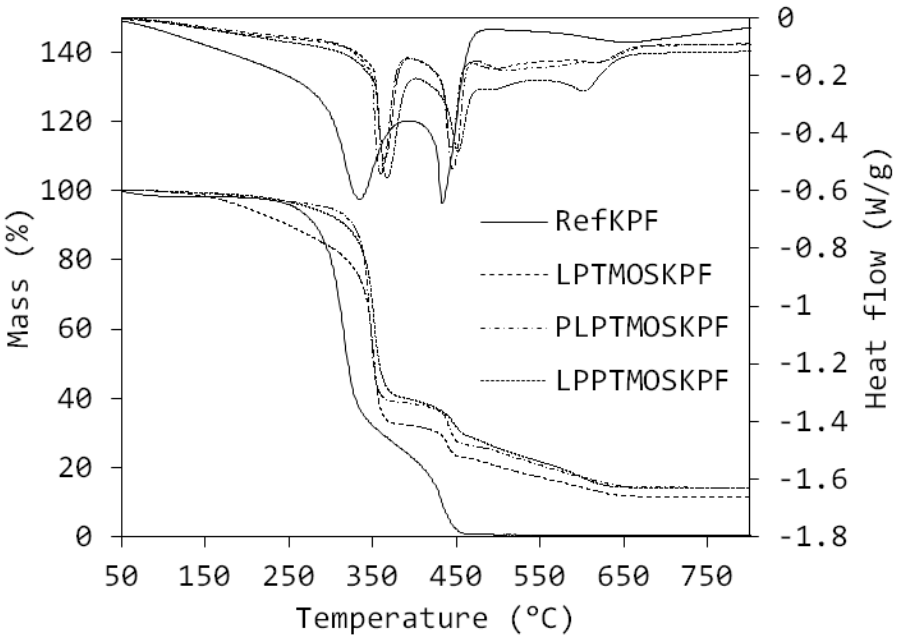

Figure 7: Thermal analysis curves of native and treated pine wood fibres showing the increased temperature resistance of all treated samples and the increased degree of precursor condensation imparted by both plasma activation and curing. Negative heat flow values indicate an exothermic process.

Infrared spectroscopy

The infrared spectra from the untreated Kraft-pulp fibres Ref_{KPF}, Figure 8, showed the expected vibrational absorption bands from wood and water, Table 2.

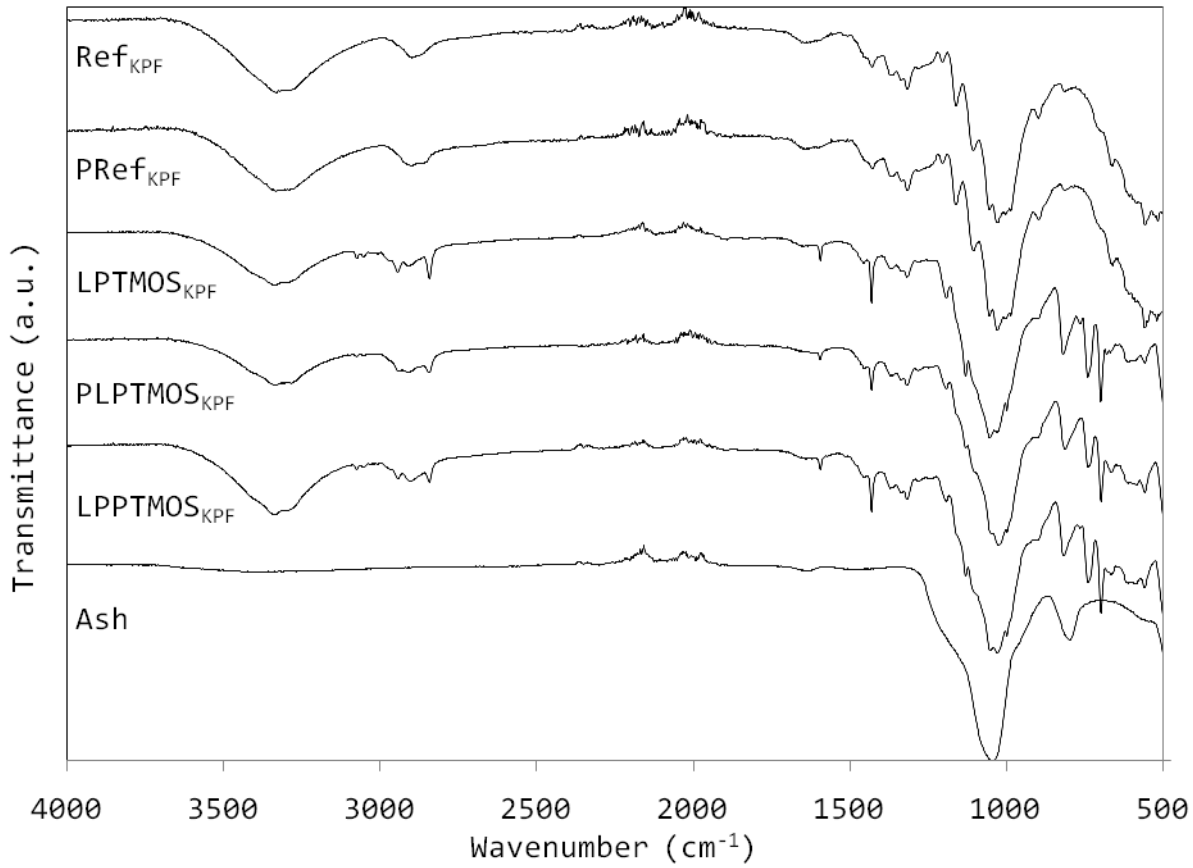

Figure 8: Infrared absorption spectra from Kraft-pulped pine wood fibres showing the inclusion of phenyl groups, silicon oxide compounds and the effect of plasma activation and curing by the removal of absorption bands assigned to methyl groups compared to $^{L}PTMOS_{W}$.

Table 2: Infrared absorption bands observed in the reference and treated KPF with R=alkyl group [9,10].

Band group	Band positions (cm^{-1})	Ref	^{P}Ref	^{L}PTMOS	^{PL}PTMOS	^{LP}PTMOS	Ash	Vibrating bond	Structural group
I	3331,3290,1640	X	X	X	X	X		O-H	H_2O, ROH
II	3073,3050,3029, 3017,3006,2872, 2841			X	X	X		C-H	R-Ph
III	3093,762			X				C-H, Si-O	OSi-Ph
IV	2896,2876	X	X					C-H	$-CH_2-$
V	2851,1456		X					C-H	$-CH_2-$
VI	2968,2942,2911			X	X	X		C-H	$-CH_3$,$-CH_2-$
VII	1594,997			X	X	X		C=C	R-Ph
VIII	1430			X	X	X		Si-C	Si-Ph
IX	1369,1362,1335, 1315	X	X	X	X	X		C-H,C-O	Cell.,Lig.
X	1280,1247,1235	X	X	X	X	X		C-C, C-O	Lig.
XI	1203	X	X					C-O	Cell.
XII	1192			X	X	X		C-O	Cell.
XIII	1160	X	X	X	X	X		C-O-C	Cell.
XIV	1129,816			X	X	X	X	Si-O	
XV	1102,1052,1028,983	X	X	X	X	X		C-C	Cell.
XVI	898,816	X	X	X	X	X		C-H	Cell.
XVII	738,732,697			X	X	X		C-H, Si-O	OSi-Ph

All non-calcined samples showed the characteristic vibrational bands assigned to water and attached –OH groups (I). They further showed the expected vibrational bands from cellulose and lignin C-H, C-O and C-C bonds motions (IX-XIII, XV, XVI). The inclusion of the phenyl groups in the liquid impregnated samples was shown by the C-H (II) and C-C vibrations (VII) assigned to aromatic groups and Si-C vibrations from attached phenyl rings (VII, VIII) [9,11,12].

In case of LPTMOS, additional OSi-Ph absorption bands (II) were found. This was assigned to residual methyl groups attached to incompletely hydrolysed precursor molecules [10]. In case of $^{PL}PTMOS_W$ and $^{LP}PTMOS_W$, these vibrations were removed. The shifts in the non-aromatic wood C-H absorption bands in the native, plasma activated and PTMOS treated samples (IV over V to VI) are indicative of chemical changes in the samples. Equally, the shift of the C-O vibrations to longer wavelengths in all treated samples (XI to XII) indicates changes in the bonding states of the hydroxyl oxygen atoms attached to wood. All treated samples showed absorption at wavelengths assigned to Si-O bonding (XIV), showing that the PTMOS molecules were deposited in the wood. More specifically, the bands at 1129 cm^{-1} are due to Si-O-Si bonds and the ones at 816 cm^{-1} to Si-OH. The deposition of silicon oxide species lead to an increase of the convoluted absorption signal around 1100 cm^{-1}, derived from asymmetric Si-O bending and overlapping the original C-O vibrations found in wood (XV). Bands at 1310 cm^{-1} and 816 cm^{-1} were assigned to wood C-H_2 wagging and rocking, respectively and did not change significantly during processing. The symmetric Si-O bending mode complexly overlaps with the C-H_2 rocking mode of cellulose, prohibiting statements about the deposited material amounts [13]. The presence of attached -OH vibrations at 1640 cm^{-1} was observed, pointing to residual incompletely condensed precursors in all treated samples.

Light- microscopy

Bright-field light micrographs from all processes showed the expected wood structure details such as the cell walls, border pits and medullary ray ports, Figure 9.

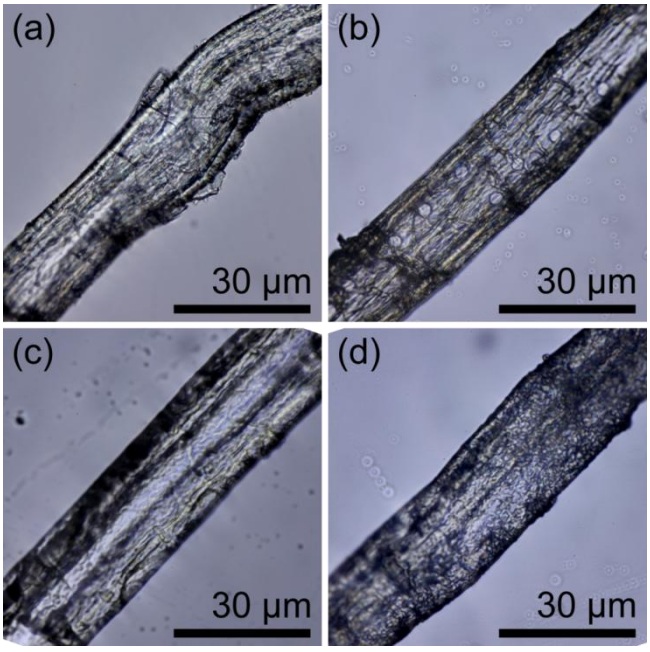

Figure 9: Light micrographs of (a) Ref_W, (b) $^{P}Ref_W$, (c) $^{L}PTMOS_W$, (d) $^{PL}PTMOS_{KPF}$ Kraft-pulp fibres.

The wood fibre ashes of Ref_{KPF} and TEOS-treated control fibres $^{L/}TEOS_{KPF}$ were strongly shrunk after calcination while those treated with PTMOS, and a control sample treated with TEOS retained their original dimensions, Figure 10. The Ref_{KPF} and $^{L/}TEOS_{KPF}$ showed strong optical anisotropy as opposed to the fibres treated with PTMOS.

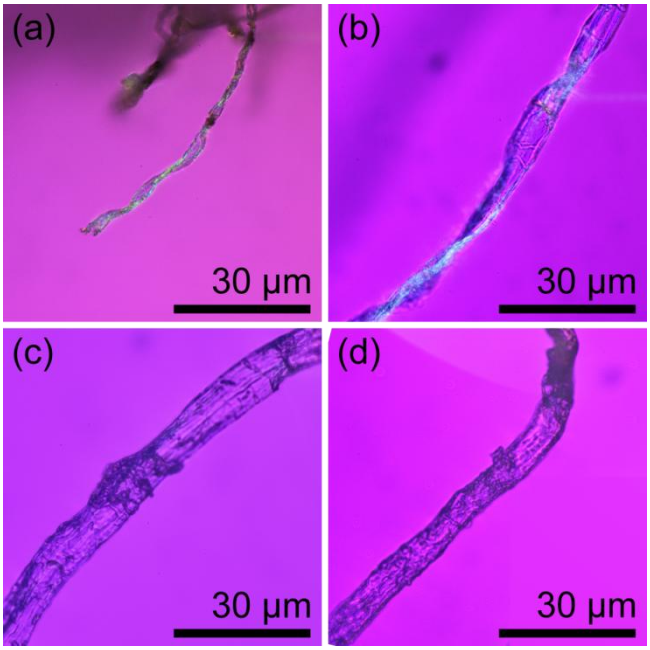

Figure 10: Polarised light micrographs with a 535 nm compensator of (a) Ref_W, (b) $^{P}Ref_W$, (c) $^{L}PTMOS_W$, (d) $^{PL}PTMOS_{KPF}$ Kraft-pulp fibre ashes.

Discussion

Argon plasma treatment

The hydrophilising effect of pure argon plasma treatment was shown by the high swelling and cracking during ASE determination as well as the particularly short contact times which prevented the measurement of the contact angle. The immediate absorption of water into $^{P}Ref_W$ is consistent with findings in literature that argon treatment creates highly polar oxycarbide species by glucose ring opening [14]. These in turn account for $^{P}Ref_W$'s high hydrophobicity.

Plasma-assisted liquid impregnation of ethanolic precursor solutions

Liquid impregnation with ethanolic PTMOS and drying in the precursor solution expectedly lead to improved water-resistance, as shown from the high ASE and contact angles of $^{L}PTMOS_W$, $^{PL}PTMOS_W$ and $^{LP}PTMOS_W$. In these three samples, the relative ASEs matched the WPG during treatment. This relation is conclusive since the main mechanism to impart ASE is cell wall pore filling. The increased ASE and contact angles from plasma activated $^{PL}PTMOS_W$ showed that the previously activated surface had indeed reacted with precursor molecules. This not only negated

the hydrophilic effect of the argon activation, but even surpassed the ASE determined of the control ^{L}PTMOS$_{W}$. In case of ^{LP}PTMOS$_{W}$, both the ASE and CA were reduced compared to ^{L}PTMOS$_{W}$ suggesting that the water-repelling effect obtained by liquid impregnation was diminished by the plasma curing. This indicates that the siloxane treatment creates resistivity against physicochemical degradation. Similarly, the shift of the exothermic wood devolatilisation mass loss from 315 °C in untreated fibres to 350 °C in all PTMOS treated fibres illustrates their higher resistance to combustion. This is due to the added inorganic/organic hybrid phase which consists of a silica network with attached, temperature-resistant phenyl groups (Van Opdenbosch et al. 2013). Their combustion takes place between 550 °C and 650 °C and is responsible for the delayed total combustion of the samples $^{L/PL/LP}$PTMOS$_{KPF}$. However, this would rule out plasma curing from the point of obtaining the highest possible water-repellence. However, most current wood paints are water-based. As shown from the reduced CA of ^{LP}PTMOS$_{W}$ with water, a hydrophilising surface treatment with argon plasma is a viable and quick route to improve wetting with such paints after liquid impregnation of PTMOS. FTIR analysis of plasma treated samples showed a change in the wood chemistry by the change of the position of the C-H vibrations and the rise of an additional absorption at 1456 cm^{-1}. The final plasma activated products had markedly reduced residual non-hydrolysed precursor methyl groups as determined by FTIR. It is most likely that the plasma activation results in a short-term activation of the wood by cleavage of C-O bonds. These may include the ether bonds of cellulose and lignin, as indicated by the aromatic smell of freshly plasma treated samples.

The inclusion of the precursors in the cell walls by ethanolic precursor impregnation was shown by light micrographs of the KPF in Figure 8 (c,d) and the volume changes of the wood pieces. It was further proven by the appearance of the ash, which was a good replica of the original fibre structure, Figure 9 (c,d). Exactly correlating the volume change of wood to the observed WPG is hampered by several circumstances. While the initial geometrical and strut densities, ϱ_{geom} (0.49 g/cm^3) and ϱ_{strut} (1.46 g/cm^3), and therefore wood porosities of 67 % are well-known, the different cell wall swellings produced by the individual processes and the unknown actual density of the material deposited within the cell walls prohibit statements about the exact precursor localisation from geometrical considerations alone. However, typical volume swellings by water of around 10 % (Mantanis, Young, and Rowell 1994) and chemically induced permanent ones up to 13 % have been reported (Zollfrank et al. 2004; Van Opdenbosch et al. 2011; Timar et al. 2000). Since such swelling is due to cell wall expansion alone, one can state that it can expand to create an internal porosity of at least 30 %. In the sample with the highest WPG of 45, ^{PL}PTMOS$_{W}$, a total volume increase by the siloxane impregnation of 11 % was found, matching expectations from earlier works [2]. In this case, the geometrically determined density $\varrho_{geom,meas}$ of 0.53 g/cm^3

also matched the expectations considering mass and volume increase: The density of the condensed precursor was determined by an Archimedic scale to be 1.27 g/cm^3. Therefore, a volume change by cell-wall bulking would lead to strut densities of 1.60 g/cm^3 and therefore the measured geometrical densities of 0.52 g/cm^3. The same holds true for ^{L}PTMOS$_{W}$ and ^{LP}PTMOS$_{W}$, meaning that the ethanolic precursors deposited mainly in the cell walls.

The fibres prepared for ash determination and FTIR had the shape of loose wool. They therefore experienced slightly different heats during drying than the flat wood pieces. The difference between the WPG of KPF and W is due to the former's higher accessible pore volume, which has been found to match that of delignified wood (Van Opdenbosch et al. 2013). However, and notably, the WPGs of ^{PL}PTMOS$_{KPF}$ were lower than those of the reference ^{L}PTMOS$_{KPF}$ and ^{LP}PTMOS$_{KPF}$. Nevertheless, the ash contents conclusively show that similar amounts of precursor were initially deposited by all fibre liquid impregnations, drying the sample in the precursor solution. Together with the findings from FTIR analysis, this supported earlier findings that the precursors deposited by ^{L}PTMOS$_{KPF/W}$ were not completely condensed after liquid impregnation and drying only [2]. Comparatively, this indicates that plasma curing indeed increased the condensation state of the precursors in the treated fibres. Plasma activation, however, lead to even stronger condensed precursors after the subsequent impregnation. The mechanism behind this phenomenon is as of yet unknown. It is proposed that the plasma leads to the creation of reactive and polar species on the wood [15]. Similar to the action of water or acids, these would increase the hydrolysis rate of the precursors. The resulting hydrolysed precursors would still be free to move and deposit within the cell walls, leading to the observed cell-wall deposition.

Additional liquid impregnations

The treatment routes using a solventless precursor were prepared to assess the possibility to omit the solvent when using prior activation of the wood surface. The samples immediately removed from the precursor solution were prepared to determine whether the amount of precursor contained within the cell lumen is sufficient to impart a significantly improved water-repellence after drying or plasma curing, respectively. Both would significantly improve the ease of processing, and therefore the economic viability of up-scaling the process of wood treatment with PTMOS.

Notably, the samples impregnated without the use of a solvent, ^{LNS}PTMOS$_{W}$ and ^{PLNS}PTMOS$_{W}$, yielded similar CA as those impregnated with ethanolic precursor solutions. Considering their lower ASE, this points to a deposition of the precursor materials on the surfaces of the cell lumen rather than within the cell walls. In agreement with its comparatively low ASE, sample ^{PLNS}PTMOS$_{W}$ showed both a low mass and comparatively lower volume increase during treatment, further confirming the surface deposition by this process. This illustrates that a solvent

with both an adequate wettability to wood and the ability to dissolve the precursor, such as ethanol, is necessary to mediate between the hydrophilic wood cell wall and the hydrophobic precursor, matching similar findings in literature [16,17]. This also explains why the additional hydrophilisation by the plasma treatment did not improve the impregnation efficiency.

On the other hand, samples dried outside the precursor solution showed comparatively high ASE. Both $^{LDO}PTMOS_W$ and $^{LDOP}PTMOS_W$ showed unexpectedly high ASE of 12 % and 11 %, respectively. This is even more significant, considering its low CA and WPG. The slightly lowered CA points to a cell wall deposition of precursors as opposed to the surface deposition observed in the samples prepared without solvent. The WPG of control sample $^{LDO}PTMOS_W$ was, due to the immediate application of vacuum, higher than that of $^{LDOP}PTMOS_W$. From the ASE of $^{LDOP}PTMOS_W$, it can be deduced that even a WPG of only 1.35 %, if deposited within the cell walls by solution impregnation, already imparts a significant wood protection by bulk modification.

Deposition from the gas phase

Although deposition of precursor was detected in the vacuum chamber, the gas-phase depositions lead to no detectable mass increase of the samples. Their ASE was expectedly 0, but the change in contact angle/-time in $^{G}PTMOS_W$ and $^{P}PTMOS_W$ with increasing treatment time indicated a small amount of surface deposition of the precursor. The short contact times of $^{PG}PTMOS_W$ match those of $^{P}Ref_W$, showing that simultaneous precursor and plasma treatment (as in $^{P}PTMOS_W$), if optimised, would be the route to impart water-repelling properties.

Influence of the surface roughness

Comparison of CA data with literature is complicated by the fact that either different wood directions than the RT (grain) direction used in this work were chosen, or the used surface and preparation method is plainly not stated [4,18]. Further, the CA is influenced by the factors (in decreasing order of magnitude) surface roughness, previous extraction treatments, moisture content and the specimen of tree analysed. We used light microscopy to assess the surface roughness of the wood pieces by focussing on three different heights: The tops of the highest fibres protruding from the wood after cutting, the height of the compact late- and earlywood fibres. From 25 measurements on five different samples, the roughness distribution was: Fibre tops 99.5±25.2 µm, compact latewood 67.3±21.3 µm, with the compact earlywood set as 0. This illustrates the typically high roughness of the wood surface after cutting, which in this work exceeds the typical fibre diameter by a factor of three. A similar approach should be followed in future works to allow for the detection of the influence of the surface roughness. The fact that the an-

gles of native wood determined in this work were higher than determined in literature by 16° is traced to this elementary issue [19].

Conclusions

The results obtained during this STSM show a marked improvement of the liquid impregnation treatment of wood with phenyl-incorporating hybrid inorganic-inorganic siloxane precursors by plasma pretreatment with regard to the condensation degree of the formed material and the resulting ASE. The effects of plasma activation, already hinted at by FTIR, will be studied in more detail by NMR and spectroscopy analysis.

The necessity of an appropriate solvent to achieve good ASE was shown, together with the high efficiency of even small amounts of precursor. The deposition locations of the precursors from the different processing routes are being confirmed in a comprehensive SEM/EDX study. This was outside the actual scope of this STSM, but will give certainty about the spatial arrangement of the components in the prepared hybrid materials. Gas phase deposition of the precursors lead to no measurable change in the wood properties.

Contact angle measurements indicate the possibility to increase the surface wettability of previously liquid impregnated wood pieces while maintaining a high ASE. This approach will be explored in near future works.

Future collaboration with host institution

It is envisioned that the possibility of plasma treatment will be further explored by varying the treatment parameters. The characterization parameters that were set down during the STSM will be used in future works to assess materials syntheses. Most importantly, the highly hydrophilising effect of argon plasma treatment will be used to improve the surface wettability of hydrophobic, bulk modified wood. This will enable the use of water-based dispersion paints on such treated wood. The proposed immediate testing will be a combined wetting and paint adhesion peeling test.

Acknowledgements

The financial support of this STSM by COST is gratefully acknowledged. In particular, the counselling of Dr. Stephanie Wieland is much appreciated. We also thank Mr Aldica for carrying out the thermal analyses.

References

1. Donath S, Militz H & Mai C. Wood modification with alkoxysilanes. Wood Science and Technology 38(7), 555–566 (2004).

2. Van Opdenbosch D, Dörrstein J, Klaithong S, Kornprobst T, Plank J, Hietala S & Zollfrank C. Chemistry and water-repelling properties of phenyl-incorporating wood composites. submitted (2013).

3. Ionita ER, Ionita MD, Stancu EC, Teodorescu M & Dinescu G. Small size plasma tools for material processing at atmospheric pressure. Applied Surface Science 255(10), 5448–5452 (2009).

4. Podgorski L, Chevet B, Onic L & Merlin A. Modification of wood wettability by plasma and corona treatments. International Journal of Adhesion and Adhesives 20(2), 103–111 (2000).

5. Stamm A, Hansen L & Seborg R. Minimizing wood shrinkage and swelling. Industrial & Engineering Chemistry 28(10), 1164–1169 (1936).

6. Elvy S, Dennis G & Ng L. Effects of coupling agent on the physical properties of wood-polymer composites. Journal of Materials Processing Technology 35(20), 3417–3419 (1995).

7. Van Opdenbosch D, Fritz-Popovski G, Paris O & Zollfrank C. Silica replication of the hierarchical structure of wood with nanometer precision. Journal of Materials Research 26(10), 1193–1202 (2011).

8. Esteves Magalhães WL & Ferreira de Souza M. Solid softwood coated with plasma-polymer for water repellence. Surface and Coatings Technology 155(1), 11–15 (2002).

9. Aloweini R, Elrassy H, Al-Oweini R & El-Rassy H. Synthesis and characterization by FTIR spectroscopy of silica aerogels prepared using several Si(OR)4 and R"Si(OR')3 precursors. Journal of Molecular Structure 919(1-3), 140–145 (2009).

10. Li Y-S, Wang Y & Ceesay S. Vibrational spectra of phenyltriethoxysilane, phenyltrimethoxysilane and their sol–gels. Spectrochimica Acta Part A: Molecular and Biomolecular Spectroscopy 71(5), 1819–1824 (2009).

11. Anderson DR. Analysis of silicones. Analysis of silicones Eds Lee Smith A, Wiley-Interscience, New York, (1974).

12. Rao A V, Kalesh RR & Pajonk GM. Hydrophobicity and physical properties of TEOS based silica aerogels using phenyltriethoxysilane as a synthesis component. Journal of Materials Science 8(21), 4407–4413 (2003).

13. Akerholm M, Hinterstoisser B & Salmen L. Characterization of the crystalline structure of cellulose using static and dynamic FT-IR spectroscopy. Carbohydr. Res. 339(3), 569–578 (2004).

14. Plasma technologies for textiles. Eds Shishoo R, Cambridge, 360 (2007).

15. Liu Y, Tao Y, Lv X, Zhang Y & Di M. Study on the surface properties of wood/polyethylene composites treated under plasma. Applied Surface Science 257(3), 1112–1118 (2010).

16. De Meijer M. Review on the durability of exterior wood coatings with reduced VOC-content. Progress in Organic Coatings 43(4), 217–225 (2001).

17. Mai C & Militz H. Modification of wood with silicon compounds. Treatment systems based on organic silicon compounds - a review. Wood Science and Technology 37(5), 339–348 (2004).

18. Podgorski L, Bousta C, Schambourg F, Maguin J & Chevet B. Surface modification of wood by plasma polymerisation. Pigment and Resin Technology 31(1), 33–40 (2001).

19. Meijer M De & Militz H. Wet adhesion of low-VOC coatings on wood A quantitative analysis. 38, 223–240 (2000).